Spectral broadening and nonlinear mode coupling in a gas-filled hollow core capillary

Olivia Zurita-Miranda, Coralie Fourcade-Dutin, P. Béjot, Frédéric Fauquet, Hervé Maillotte, Patrick Mounaix, Damien Bigourd

Spectral broadening and nonlinear mode coupling in a gas-filled hollow core capillary

Olivia Zurita-Miranda[1,2], Coralie Fourcade-Dutin[1], Pierre Béjot[3], Frédéric Fauquet[1], Hervé Maillotte[2], Patrick Mounaix[1], Damien Bigourd[1*]

[1*]Laboratoire IMS, UMR5218 CNRS, University of Bordeaux, 33400 Talence, France.
[2]Institut FEMTO-ST, Département Optique, UMR 6174, Université Bourgogne Franche-Comté-CNRS, 25030 Besançon, France.
[3]Laboratoire Interdisciplinaire Carnot de Bourgogne, UMR6303 CNRS-UBFC, 21000 Dijon, France.

*Corresponding author(s). E-mail(s): damien.bigourd@u-bordeaux.fr;

Abstract

In this investigation, we explore the phenomenon of spectral broadening in a gas-filled hollow-core capillary induced by ultra-short pulses, with a focus on nonlinear mode coupling **at a power lower than the critical power**. As the pulse propagates through the capillary, the spectrum primarily broadens due to self-phase modulation, and concurrently, high-order modes are generated through interactions between different modes. Both experimental and numerical results consistently demonstrate that the spectral region near the center of the spectrum remains within the fundamental mode, while the spectral edges propagate in higher-order modes, predominantly in the LP_{12} mode generated through nonlinear mode coupling within the gas-filled hollow-core capillary. This observation is relatively weak but is of paramount importance for the design of post-compression systems in gas-filled hollow-core capillaries with a high-quality beam profile **when the power starts to reach the critical level**. Understanding and then accommodating the dynamics of nonlinear mode coupling are crucial for achieving the desired characteristics and beam quality while optimising the performance of such systems.

Keywords: Nonlinear mode coupling, hollow core capillary, spectral broadening

1 Introduction

Hollow core capillaries (HCC) filled with gas have found widespread use as a platform for converting light through nonlinear processes. One of the most commonly employed techniques involves compressing extremely short, high-energy laser pulses [1–7]. During this process, the input pulse undergoes spectral broadening primarily due to self-phase modulation and afterward, the pulse is compressed using phase compensators, ultimately achieving a few-cycle duration. Gas-filled HCC have also been integrated into various optical nonlinear studies, including investigations into **soliton and dispersive wave generation [8–13] and four-wave-mixing [14–19]**, among others. Nowadays, there is a renewed interest in nonlinear interaction within multimode waveguides providing a new degree of freedom for nonlinear conversion. For example, it is possible to reach the

anomalous dispersive regime for high order modes (HOM) while the fundamental mode lies in the normal dispersion regime. Particularly, it leads to the generation of various phenomena, like other types of solitons [20, 21], conical waves [22], dispersive waves [23], few cycle pulses [24] in multimode waveguides, to mention just some examples. Alternatively, the amazing control of the beam, now achievable, allows to tailor the spatiotemporal properties of the input beam shape to synthesize ultrafast wavepackets [25] before injecting them into the HCC, thereby directly exciting specific HOM. The generation of HOM is often achieved through nonlinear spatiotemporal coupling due to intense light propagation in a gas and controlled via parameters influencing the nonlinear process [**26**–**29**]. Spatial kerr effect [30] or ionization process [31] within the HCC reshapes the propagating light and create new spectral components. The intensity dependent refractive index causes self-focusing of the beam toward the more intense central region of the HCC, which activates high order modes during propagation. This effect typically occurs when the input peak power exceeds or approaches a critical power threshold (P_c) required to transfer energy from the fundamental mode to HOM [26, 27]. It has also been demonstrated that light confinement in the HCC can induce spatial collapse, possibly occurring below this critical value due to a complex spatio-temporal dynamic **with a power equals to 0.86 times the critical power** [27]. While this nonlinear mode mixing can be very advantageous to achieve intense few-cycle pulses [24], it may impede the overall performance of conventional post-compression techniques designed for single mode output, in addition to the intrinsic difficulties in managing dispersion and non linearity over a broad bandwidth. **In this manuscript, the generation of HOM resulting from the nonlinear interaction with spatio-temporal coupling is experimentally and numerically investigated at a power below the critical level. In this configuration, HOM are usually not observed and may be weak. Here, we propose to focus on this observation and origins. We adopt a standard configuration** where the input spectrum undergoes broadening, mostly due to self-phase modulation, as it propagates through an Argon-filled HCC. In the resulting spectrum, the central spectral region has a distinct bell-like shape reminiscent of the LP_{01} mode while the spectral edges exhibit HOM. The goal of this experimental and numerical study is to explore and characterize the spectral and spatio-temporal nonlinear dynamics of HOM coupling, so as to finely control ultra-short pulse propagation in the HCC.

2 Experimental results

The experimental setup, as illustrated in Figure 1, involves a Ti:Sa amplifier system (Libra, Coherent Inc.) that generates pulses with a duration of approximately 120 fs at full width at half maximum (FWHM). These pulses are delivered at a repetition rate of 1 kHz, and the maximum pulse energy reaches around 800 μJ, with the spectrum centered at 805 nm. The pulses are injected with a lens (f=500 mm) into a 30 cm-long HCC featuring an inner diameter of 150 µm, located in a home-made metal chamber. Then, the output beam is collimated using a lens with a focal length of 150 mm and is characterized with spectrometers and two cameras that record both far-field and near-field images. The initial measurements were taken when the HCC was under vacuum conditions, as depicted in Figure 2.a. The spectrum exhibited a spectral bandwidth of 8 nm, and the near-field and far-field images closely resembled the profile of the LP_{01} mode due to the optimized alignment of the HCC. Subsequently, the chamber and the HCC were filled with Argon gas, reaching a gas pressure (P_{gas}) equals to approximately 4 bar. This pressure leads to the propagation of the fundamental mode in the normal dispersion regime.

When the pump peak power is set at approximately 1.61 GW (**$\approx P_c/6$, for an energy of 205 µJ**), the pump spectrum broadens mostly due to self-phase modulation and self-steepening, and extends to a wavelength lower than 680 nm and higher than 875 nm (Figure 2.c in a linear scale). To efficiently detect the weak spectral part on the edges, the entire spectrum was selectively filtered so as to appropriately isolate the edges from the central zone. We employed a short-pass filter with a cut-off wavelength of 650 nm (Thorlabs-FES0650), a high-pass filter with a cut-off wavelength of 900 nm (Thorlabs, FELH0900), and a bandpass filter centered at 800 nm. These filters allowed us to examine the spectrum at shorter

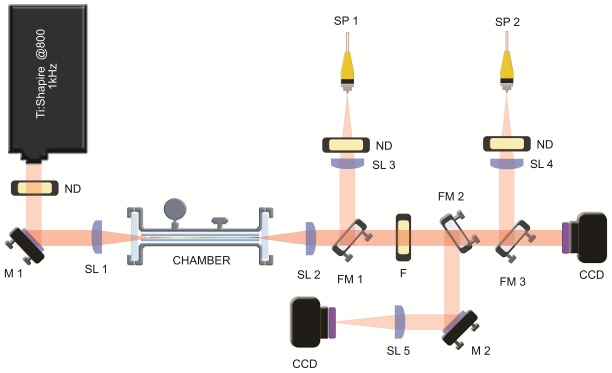

Fig. 1 Experimental set-up. M, Mirror, SL Plano Convex lens, ND absorptive neutral density filter, F, Filters, FM, Flip Mirror, CCD Camera, SP1, Spectrometer 1 , SP2, Spectrometer 2.

wavelengths (SW), longer wavelengths (LW), or the central (CW) region, in conjunction with the near-field and far-field profiles. The shape of the filtered beam at the CW region (Figure 2.b) is notably circular, as depicted in Figure 2.f and 2.g, and closely resembles a LP_{01} mode, similar to what was observed under vacuum conditions (see Figure 2.d and 2.e).

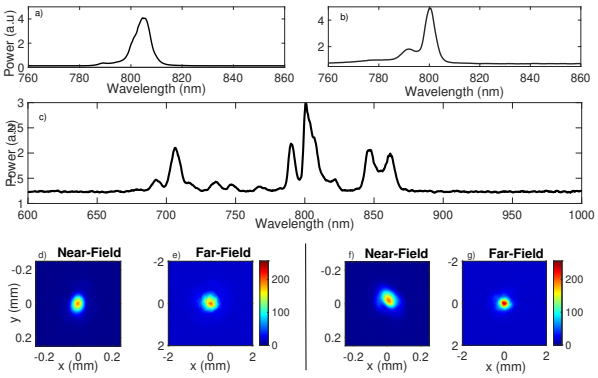

Fig. 2 a) Input spectrum b) Filtered central region of the output spectrum c) Output spectrum when the pulses propagate in a 30 cm-long HCC. The pressure is approximately 4 bar and the peak power is 1.61 GW d-e) Far-field and near-field images **of the output beam with the HCC under vacuum** f-g) Far-field and near-field images of the output beam.

The filtered spectra at SW and LW are presented in Figure 3.a and 3.b. Since the central part of the spectrum was removed by the filter,

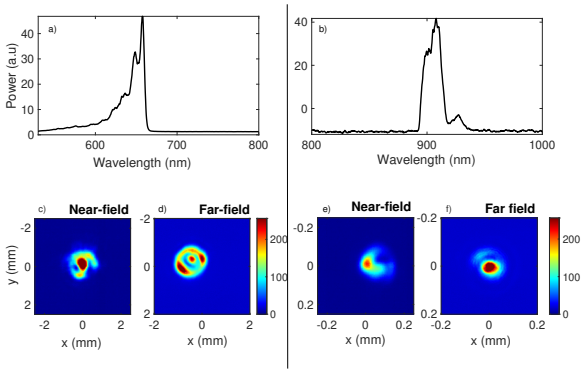

Fig. 3 a-b) Filtered spectra at SW and LW with an increase power in front of the spectrometer c-f) Images of the near and far field for each filtered spectrum

the total power was lower. Thus, we increased the input power in front of the spectrometers by changing the neutral density to observe the spectral edges at approximately 650 nm and 900 nm, unseen in Figure 2.c. The beam profiles corresponding to SW and LW, as seen in Figure 3.c-d and Figure 3.e-f, display multiple structures and highlight that the fundamental mode is not predominant in the filtered spectra. We anticipate that the recorded beam profiles are the result of a combination of several beam profiles within the filter bandwidth, including modes such as LP_{01} and LP_{02}. **In this configuration,** this nonlinear coupling of modes is primarily observed at the spectral edges, owing to the spatio-temporal interaction during the propagation within the gas-filled HCC.

3 Numerical results

To gain a more comprehensive understanding of the impact of the nonlinear mode coupling **at low power** within the gas filled HCC, simulations were conducted by solving the generalized unidirectional pulse propagation equation expressed in the modal basis. **The modes in a capillary are theroretically described with hybrid electromagnetic HE modes. Nevertheless, we approximate the real vectorial modes by their scalar counterparts, LP modes, in the weak guidance approximation.** The equation incorporates factors such as the transversal distribution of the refractive index, modal linear

dispersion, the Kerr effect [32, 33]. **The nonlinear refractive index of $10^{-23}m^2$/W has been taken** It also incorporates the ionisation process even if it has no contribution in the current investigation. **The loss of the capillary has been ignored to save some computation time. As the losses of the HOM should be higher [31], their observations are slightly overestimated in the simulation compared to the fundamental mode**. Then, we performed nonlinear propagation simulations in which 120-fs Gaussian pulses propagated in the 30 cm long HCC filled with Argon gas at a pressure gas of 4 bar. The beam waist of the input beam is set at ω_r**=57 µm (FWHM)** to maximize the HCC coupling in the fundamental mode. The spectrum was initially recorded as the function of the HCC length in the logarithmic scale (Figure 4). As anticipated, the spectrum experiences gradual broadening during propagation, predominantly due to self-phase modulation. The spectrum reaches wavelengths higher and lower than 900 nm and 650 nm, respectively, as in the experimental observation (Figure 2 and Figure 3). Concurrently, there is an oscillation of the peak fluence throughout the propagation, indicating that the laser beam undergoes spatial stretching and compression along its length (Figure 5). The nonlinearity provides efficient power transfer to HOM, as in self-focusing condition. This spatio-temporal coupling is primarily from the fundamental mode to an ensemble of HOM [26, 30]. The HOM are populated from the modal four-wave mixing process along the propagation from the product between the spatial modes present in the HCC [30]. However the LP_{01} and LP_{02} modes are mostly coupled due to the smaller phase-mismatch between their wave-vectors. The noisy-like shape is actually due to the interaction of an ensemble of modes. However, the main oscillation corresponds to the power transfer between these two LP_{01} and LP_{02} modes and the period is directly linked to the coherence length $L_c = 2\pi/(\beta_{11} - \beta_{12})$ with β_{11} and β_{12} the wave vectors of these two first modes. In our conditions, L_c equals approximatively to ≈2.25 cm and this value aligns well with the period obtained in Figure 5. Simultaneously to this modal transfer, new frequencies are generated from the self-phase modulation and intermodal cross-phase modulation. As the fundamental mode is the strongest, it acts predominantly in the nonlinear processes to broaden the spectrum and generates the HOM [24].

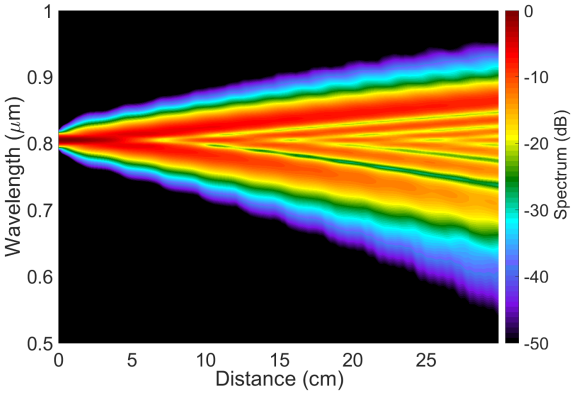

Fig. 4 Numerical calculation of the spectral broadening as the function of the HCC length in the logarithmic scale.The Argon pressure is 4 bar.

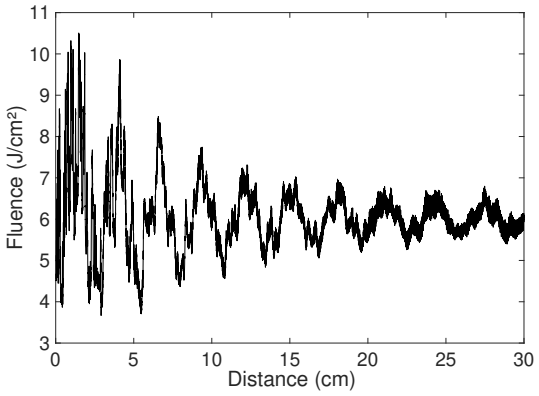

Fig. 5 Fluence as the function of the HCC length exhibiting the couplings between the modes. The beating of the two first LP_{01} and LP_{02} modes has a period of 2.25 cm.

Figure 6 illustrates the mode resolved spectrum at the HCC output as the function of the radial coordinates. The stronger contribution of the spectral broadening is mostly originated from the fundamental mode even if HOM exists across the full spectrum. It means than the beam profile in the middle part of the spectrum will exhibit a shape close to the fundamental mode, as observed

in the experiment. When approaching the edge of the spectrum, the contribution of HOM becomes stronger relatively to the one of the fundamental mode. For example the LP_{02} exhibits a stronger contribution for a wavelength higher than 910 nm or lower than 630 nm. To summarize this part, the relative contribution of HOM versus the fundamental mode depends on the spectral selection at the HCC output. It emphasizes that the beam profile, observed on a camera, strongly depends of the chosen wavelength range of the mode distribution.

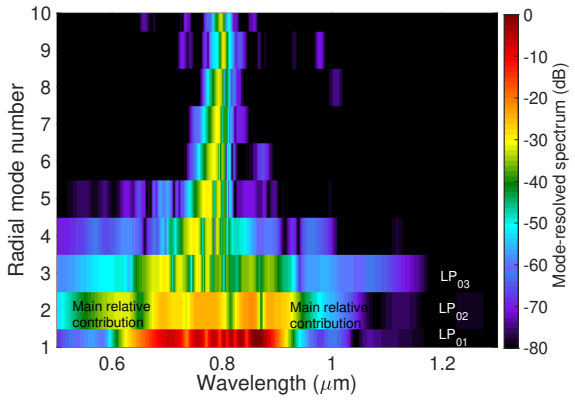

Fig. 6 Mode resolved spectrum at the HCC output as the function of the function of radial mode order.

The beam profiles for several spectral region were plotted to compare the numerical simulation at the HCC output with experimental results. As shown in Figure 7.a, the beam profile in the middle of the spectrum exhibits a clear LP_{01} shape, confirming that HOM are weakly present in this spectral part relative to the fundamental mode. The SW and LW portions of the spectrum were then selected using the cut-off wavelengths of 620 and 930 nm, similarly to the experimental procedure. The corresponding, spectrally integrated, beam profiles are presented in Figure 7.b and c. In the SW region, the beam displays a distinct ring, supporting the presence of HOM, particularly the LP_{02} mode. Similarly, the beam in the LW part also exhibits a ring shape, resulting from the contribution of HOM. We also checked that when a small asymmetry is applied to the input beam, an asymetry is observed at the HCC output

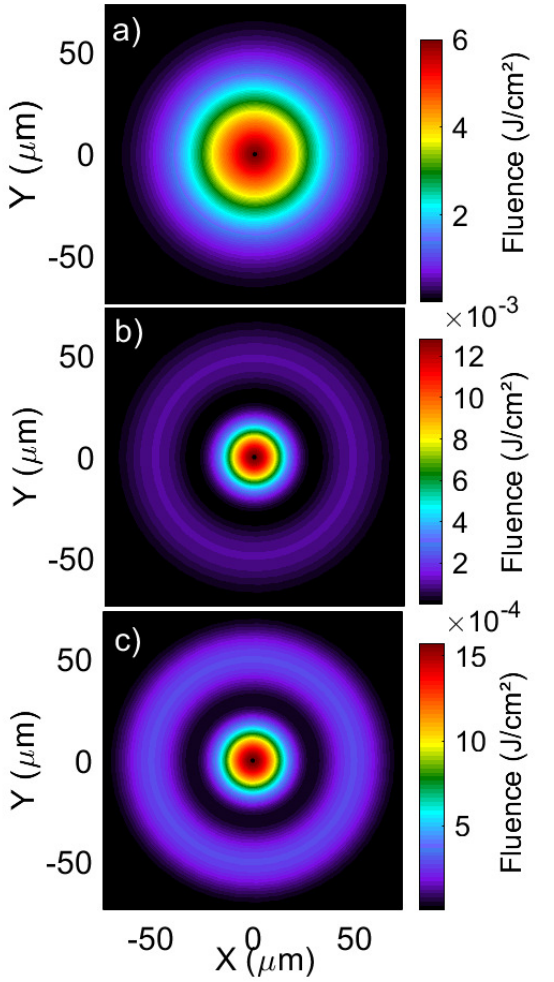

Fig. 7 Beam profiles when the filter selects a) the middle part, b) the SW with a cut-off wavelength of 620 nm or c) the LW portions of the spectrum with a cut-off wavelength of 930 nm

attributed to the weak azimuthal mode content. In fact, this explains partly the observed assymetric beam profile in the experiment (Figure 3). In addition, the quality of the experimental beam profiles are subject to other various experimental constraints, such as the input beam shape, focusing conditions, quality of the HCC and alignment of the detection scheme. Nevertheless, **in this regime at low power,** the simulation leads to the same conclusion : the spectral portion close to the center remains within the LP_{01} mode, while the edge propagates in HOM, mostly in the LP_{02} mode, generated through the nonlinear mode coupling in the gas-filled HCC.

4 Conclusion

We highlighted the generation of HOM at the edge of the broadened spectrum due to a nonlinear mode coupling. Both experimental and numerical results consistently demonstrate that **in our condition at low power** the spectral region near the spectrum center remains within the LP_{01} mode, while the edges correspond to the generated HOM propagation, primarly in the LP_{02} mode generated through nonlinear mode coupling in the gas filled HCC. This observation holds significant importance in the design considerations for a post-compression system in gas-filled HCC **when the HOM becomes predominant at higher power**. Understanding and accounting for the dynamics of nonlinear mode coupling are critical elements in optimizing the performance of such systems for achieving the desired pulse characteristics and beam quality.

Declarations

- This work was supported by the IdEx University of Bordeaux / Grand Research Program LIGHT (contract ANR 10-IDEX-0003). The authors also acknowledge financial support of French programs "Investments for the Future" operated by the National Research Agency (ISITE-BFC, contract ANR-15-IDEX-03; EIPHI Graduate School, contract ANR-17-EURE-0002; EQUIPEX+ Smartlight, contract ANR-21- ESRE-0040), from Bourgogne Franche-Comté region and European Regional Development
- The authors declare no conflicts of interest.
- Data underlying the results presented in this paper are not publicly available at this time but may be obtained from the authors upon reasonable request.

References

[1] M. Nisoli, S. De Silvestri, O. Svelto, R. Szipöcs, S. Szipöcs, K. Ferencz, C. Spielmann, S. Sartania, F. Krausz, Compression of High-Energy Laser Pulses below 5 fs. Optics Letters **22** (8), 522-524 (1997).

[2] C. Fourcade-Dutin, A. Dubrouil, S. Petit, E. Mével, E.Constant, D.Descamps, Post-compression of high-energy femtosecond pulses using gas ionization. Optics Letters **35** (2), 253-255 (2010).

[3] P. Béjot, B. E. Schmidt, J. Kasparian, J.-P. Wolf, F. Legaré, Mechanism of hollow-core-fiber infrared-supercontinuum compression with bulk material. Physical Review A **81** 063828 (2010).

[4] B. E. Schmidt, P. Béjot, M. Giguère, A. D. Shiner, C. Trallero-Herrero, E. Bisson, J. Kasparian, J-P. Wolf, D. M. Villeneuve, J-C. Kieffer, P. B. Corkum, F. Légaré, Compression of 1.8 m laser pulses to sub two optical cycles with bulk material. Applied Physics Letters **96** 121109 (2010).

[5] G Fan, PA Carpeggiani, Z Tao, G Coccia, R Safaei, E Kaksis, A Pugzlys, F Légaré, BE Schmidt, A Baltuška, 70 mJ nonlinear compression and scaling route for an Yb amplifier using large-core hollow fibers. Optics Letters **46** 896-899 (2021).

[6] T. Nagy, P. Simon, L. Veisz, High-energy few-cycle pulses: post-compression techniques. Advances in Physics X **6:1** 1845795 (2020).

[7] T. Nagy, L. von Grafenstein, D. Ueberschaer, U. Griebner, Femtosecond multi-10-mJ pulses at 2 µm wavelength by compression in a hollow-core fiber. Optics Letters **46** 3033-3036 (2021)

[8] T. Balciunas, C. Fourcade-Dutin, G. Fan, T. Witting, A. A. Voronin, A. M. Zheltikov, F. Gerome, G. G. Paulus, A. Baltuska, F. Benabid, A strong-field driver in the single-cycle regime based on self-compression in a kagome fibre. Nature Communication **6:6117**, 1-7 (2015).

[9] J. C. Travers, Optical solitons in hollow-core fibres. Optics Communication **555** 130191 (2024)

[10] F. Köttig, D. Schade, J. R. Koehler, P. St. J. Russell, F. Tani, Efficient single-cycle pulse compression of an ytterbium fiber laser at 10

MHz repetition rate. Optics Express **28** 9099-9110 (2020)

[11] J. C. Travers, T. F. Grigorova, C. Brahms, F. Belli, High-energy pulse self-compression and ultraviolet generation through soliton dynamics in hollow capillary fibres. Nature Photonics **13**, 547-554 (2019).

[12] M. Reduzzi, M. Pini, L. Mai, F. Cappenberg, L. Colaizzi, F. Vismarra, A. Crego, M. Lucchini, C. Brahms, J. C. Travers, R. Borrego-Varillas, M. Nisoli, Direct temporal characterization of sub-3-fs deep UV pulses generated by resonant dispersive wave emission. Optics Express **31** 26854-26864 (2023).

[13] C. Zhang, T. Chen, J. Pan, Z. Huang, D. Liu, D. Wang, F. Yu, D. Wu, Y. Zheng, R. Yin, X. Jiang, M. Pang, Y. Leng, R. Li, Measurements of microjoule-level, few-femtosecond ultraviolet dispersive-wave pulses generated in gas-filled hollow capillary fibers. Optics Letters **47** 4830-4833 (2022).

[14] F. Belli, A. Abdolvand, J. C. Travers, P. St. J. Russell, Highly efficient deep UV generation by four-wave mixing in gas-filled hollow-core photonic crystal fiber. Optics Letters **44** (22), 5509-5512 (2019).

[15] O. Zurita-Miranda, C. Fourcade-Dutin, F. Fauquet, F. Darracq, J.-P. Guillet, P. Mounaix, H. Maillotte, D. Bigourd, Tunable ultrafast infrared generation in a gas-filled hollow-core capillary by a four-wave mixing process. Journal of the Optical Society of America B **39** (3), 662-670 (2022).

[16] C. Fourcade-Dutin, O. Zurita-Miranda, P. Mounaix, D. Bigourd, Mid-infrared ultra-short pulse generation in a gas-filled hollow-core photonic crystal fiber pumped by two-color pulses. Fibers **9** (4), 1-9 (2021).

[17] A. G. Ciriolo, A. Pusala, M. Negro, M. Devetta, D. Faccialà, G. Mariani, C. Vozzi, S. Stagira, Generation of ultrashort pulses by four wave mixing in a gas-filled hollow core fiber. Journal of Optics **20** 125503 (2018).

[18] D. Faccio, A. Grün, P. K. Bates, O. Chalus, J. Biegert, Optical amplification in the near-infrared in gas-filled hollow-core fibers. Optics Letters **34** 2918–2920 (2009).

[19] Y. Kida, T. Imasaka, Optical parametric amplification of a supercontinuum in a gas. Applied Physics B **116**, 673–680 (2014).

[20] B. A. López-Zubieta, E. C. Jarque, Í. J. Sola, J. S. Roman, Spatiotemporal-dressed optical solitons in hollow-core capillaries. OSA Continuum **1**(3), 930-938 (2018).

[21] Y. Wan, W. Chang, Spatiotemporal-dressed optical solitons in hollow-core capillaries. Optics Express **29** 7070-938 (2021).

[22] B. Kibler, P. Béjot, Discretized Conical Waves in Multimode Optical Fibers. Physical Review Letters **126**, 023902 (2021).

[23] C. Brahms, J. C. Travers, Soliton self-compression and resonant dispersive wave emission in higher-order modes of a hollow capillary fibre. Journal of Physics : Photonics **4**, 1-10 (2022).

[24] R. Piccoli, J. M. Brown, Y. G. Jeong, A. Rovere, L. Zanotto, M. B. Gaarde, F. Légaré, A. Couairon, J. C. Travers, R. Morandotti, B. E. Schmidt, L. Razzari, Intense few-cycle visible pulses directly generated via nonlinear fibre mode mixing. Nature Photonics **15**, 884-889 (2021).

[25] D. Cruz-Delgado, S. Yerolatsitis, N. K. Fontaine, D. N. Christodoulides, R. Amezcua-Correa, M. A. Bandres, Synthesis of ultrafast wavepackets with tailored spatiotemporal properties. Nature Photonics **16**, 686-691 (2022).

[26] G. D. Hesketh, F. Poletti, P. Horak, Spatio-Temporal Self-Focusing in Femtosecond Pulse Transmission Through Multimode Optical Fibers. Journal of Lightwave Technology **30**(17), 2764-2769 (2012).

[27] A. Crego, E. Conejero Jarque, J. San Roman, Influence of the spatial confinement on the self-focusing of ultrashort pulses in hollow-core

fibers. Scientific Reports **9:9546**, 1-12 (2019).

[28] M. Kumar, M. Arshadipirlar, R. Safaei, H. Ibrahim, F. Légaré, Generating ultrashort visible light pulses based on multidimensional solitary states in gas-filled hollow core fiber. APL Photonics **8**(5), 056104 (2023)

[29] 1. R. Safaei, G. Fan, O. Kwon, K. Légaré, P. Lassonde, B. E. Schmidt, H. Ibrahim, F. Légaré, High-energy multidimensional solitary states in hollow-core fibres, Nature Photonics **14**(12), 733–739 (2020).

[30] G. Tempea, T. Brabec, Theory of Self-Focusing in a Hollow Waveguide. Optics Letters **23**(10), 762-764 (1998).

[31] T. Auguste, O. Gobert, C. Fourcade-Dutin, A. Dubrouil, E. Mével, S. Petit, E. Constant, D. Descamps, Application of Optical-Field-Ionization-Induced Spectral Broadening in Helium Gas to the Post-compression of High-Energy Femtosecond Laser Pulses. Journal of the Optical Society of America B **29**(6)-, 1277-1286 (2012).

[32] P. Béjot, Multimodal unidirectional pulse propagation equation. Physical Review E **99**, 032217 (2019).

[33] K. Tarnowski, S. Majchrowska, P. Béjot, B. Kibler, Numerical modelings of ultrashort pulse propagation and conical emission in multimode optical fibers. Journal of the Optical Society of America B **38**, 732-742 (2021).